THE JOURNAL OF BIOLOGICAL CHEMISTRY VOL. 281, NO. 8, pp. 5149–5157, February 24, 2006
Printed in the U.S.A.

The Nuclear Import of Protein Kinase D3 Requires Its Catalytic Activity*

Received for publication, July 22, 2005, and in revised form, December 5, 2005 Published, JBC Papers in Press, December 27, 2005, DOI 10.1074/jbc.M508014200

Osvaldo Rey[‡1], Romeo Papazyan[‡], Richard T. Waldron[‡], Steven H. Young[‡], Jennifer Lippincott-Schwartz[§], Rodrigo Jacamo[‡], and Enrique Rozengurt[‡2]

From the [‡]Unit of Signal Transduction and Gastrointestinal Cancer, Division of Digestive Diseases, Department of Medicine, CURE Digestive Diseases Research Center and Molecular Biology Institute, David Geffen School of Medicine, University of California, Los Angeles, California 90095 and the [§]National Institute of Child Health and Human Development, Cell Biology and Metabolism Branch, National Institutes of Health, Bethesda, Maryland 20892

The protein kinase D (PKD) family consists of three serine/threonine protein kinases termed PKD, PKD2, and PKD3, which are similar in overall structure and primary amino acid sequence. However, each isozyme displays a distinctive intracellular localization. Taking advantage of the structural homology and opposite nuclear localization of PKD2 and PKD3, we generated an extensive set of chimeric proteins between both isozymes to determine which PKD3 domain(s) mediates its nuclear localization. We found that the C-terminal region of PKD3, which contains its catalytic domain, is necessary but not sufficient for its nuclear localization. Real time imaging of a photoactivatable green fluorescent protein fused to PKD3 revealed that point mutations that render PKD3 catalytically inactive completely prevented its nuclear import despite its interaction with importin α and β. We also found that activation loop phosphorylation of PKD3 did not require its nuclear localization, and it was not sufficient to promote the nuclear import of PKD3. These results identify a novel function for the kinase activity of PKD3 in promoting its nuclear entry and suggest that the catalytic activity of PKD3 may regulate its nuclear import through autophosphorylation and/or interaction with another protein(s).

The protein kinase D (PKD)[3] family consist of three serine/threonine protein kinases termed PKD, PKD2, and PKD3 with structural, enzymological and regulatory properties different from the protein kinase C (PKC) family (1–5). The N-terminal regulatory portion of the different members of the PKD family contains a cysteine-rich domain (CRD) comprising a tandem repeat of cysteine-rich zinc-finger like motifs, termed cys1 and cys2, that confers high affinity binding to phorbol esters and DAG followed by a pleckstrin homology (PH) domain that regulates catalytic activity (6–9). The C-terminal region of the PKDs contains its catalytic domain, which is distantly related to Ca^{2+}-regulated kinases (1).

PKDs can be activated in intact cells by pharmacological agents such as biologically active phorbol esters and physiological stimuli including G protein-coupled receptor (GPCR) agonists, growth factors and antigen-receptor engagement (10). In all cases, activation involves a PKC-dependent phosphorylation of two serine residues within the PKD activation loop (5, 10–12). PKD, the most extensively studied member of this family of kinases, has been implicated in the regulation of a variety of cellular functions, including DNA synthesis and cell proliferation, chromatin modification, Golgi organization and function, c-Jun signaling, NFκB-mediated gene expression, and cell migration (reviewed in Ref. 10).

Increasing experimental evidence support the notion that the targeting of signaling molecules to different cellular compartments is a fundamental process in the regulation of their activity (13–15). In the case of the PKD isozymes, several studies have demonstrated that despite their extensive structural homology, their intracellular distribution is notably different. PKD, which has been localized in the cytosol and in several intracellular compartments including the Golgi and mitochondria (16–19), undergoes a rapid intracellular redistribution in response to GPCR agonists. This process includes a reversible translocation from the cytosol to the plasma membrane and a transient nuclear accumulation. At least two domains located in the N-terminal region of PKD, *i.e.* the cys2 of the CRD and the PH domain, mediate its nuclear import and export, respectively (19–22). PKD2 is a cytoplasmic protein that also undergoes a reversible plasma membrane translocation in response to GPCR agonists (23, 24). In contrast to PKD and PKD2, it has been established that PKD3 is present in both the nucleus and cytoplasm of unstimulated fibroblast and epithelial cells (5).

Taking advantage of the structural homology and opposite nuclear localization of PKD2 and PKD3 in unstimulated cells, we generated a set of chimeras between these isozymes to determine which PKD3 domain(s) mediates its nuclear localization. A chimeric protein comprising the regulatory N-terminal region of PKD3 and the C-terminal region of PKD2, which includes its catalytic domain, displayed a cytoplasmic distribution indistinguishable from wild type (wt) PKD2. Conversely, when the C-terminal region of wt PKD2 was replaced with the equivalent region of PKD3, the resulting protein displayed the same intracellular distribution as wt PKD3, *i.e.* nuclear and cytoplasmic. Further analysis demonstrated that point mutations that render PKD3 catalytically inactive completely prevented its nuclear import but not its activation loop phosphorylation. Collectively, these results indicate a novel function for the kinase activity of PKD3 in promoting its nuclear entry and suggest that the catalytic activity of PKD3 regulates its nuclear transport through autophosphorylation and/or interaction with another protein(s).

* This work was supported by National Institutes of Health Grants DK 55003 and DK 56930 (to E. R.) and K01CA097956 (to O. R.) and by the Morphology/Imaging Core of the CURE Center Grant 5 P30 DK41301. The costs of publication of this article were defrayed in part by the payment of page charges. This article must therefore be hereby marked "*advertisement*" in accordance with 18 U.S.C. Section 1734 solely to indicate this fact.

[1] To whom correspondence should be addressed: 900 Veteran Ave., Warren Hall Rm. 11-115, Dept. of Medicine, David Geffen School of Medicine, University of California at Los Angeles, Los Angeles, CA 90095-1786. Tel.: 310-794-5902; Fax: 310-267-2399; E-mail: orey@mednet.ucla.edu.

[2] The Ronald S. Hirshberg Professor of Translational Pancreatic Cancer Research.

[3] The abbreviations used are: PKD, protein kinase D; CRD, cysteine-rich domain; DAG, diacylglycerol; GFP, green fluorescent protein; GPCR, G protein-coupled receptor; PBS, phosphate-buffered saline; TRITC, tetramethylrhodamine isothiocyanate; LMB, leptomycin B; NT, neurotensin; PAGFP, photoactivatable GFP; PDBu, phorbol 12,13-dibutyrate; PH, pleckstrin homology domain; PKC, protein kinase C; RFP, red fluorescent protein; wt, wild type.

EXPERIMENTAL PROCEDURES

Plasmids—Site-directed mutagenesis, performed as previously described (19), was used to engineer point mutations and restriction sites flanking the CRD, PH, and catalytic domain of PKD2 and PKD3 to generate the different plasmids. The forward (displayed) and complementary primers (not shown) used were: PKD2-CRD PacI site, 5-GCCACCTTCGAGGACTTCCAGTTAATTAACATCCGCCC-GCACGCC-3; PKD2-CRD AscI site, 5-CCTTGGAGAGGTTACT-GGCGCGCCCTTCAATGGAGAACC-3; PKD2-PH PvuI site, 5-GCGACACACGACGCGGCGATCGAGCACCACGCTGCGG-3; PKD2-PH PmeI site, 5-GCCCCAGGCCCTGATGTTTAAACCCG-TCATCCTTCAGG-3; PKD2-catalytic domain PacI site, 5-GCATC-TCTGTGTCCTTAATTAATAGTCAGATCCAACAG-3; PKD3-CRD PacI site, 5-GAAGACTTCCAGTTAATTAACATTCGTCC-ACATAAC-3; PKD3-CRD AscI site, 5-CCTTGGAGAGGTTACT-GGCGCGCCCTTCAATGGAGAACC-3; PKD3-PH PvuI site, 5-CCATCAAGCACACAAAGAGGCGATCGAGCACAATGGTGA-AGG-3; PKD3-PH PmeI site, 5-CGCCAAGCCCTCATGTTTAAA-CCTGTTACTCCCTCAAGC-3 and PKD3-catalytic domain PacI site, 5-GTATCTCTGTATCTTTAATTAATTGTCAGATTCAGG. After the generation of the restriction sites, the resulting cDNAs for PKD2 and PKD3 were digested to isolate the different domains, which were then subcloned into the alternative cDNA. For example, after isolating the CRD of PKD3 using PacI and AscI, the DNA fragment was moved into the cDNA of PKD2 previously digested with the same enzymes. To delete the Cys2 domain of PKD3, two AscI sites were engineered at the 5′- and 3′-regions flanking this domain using the forward (displayed) and complementary primers (not shown) 5-GCAGAGTGAAAGTTGGCGCGCCCCACACATTT-GC-3 and 5-CCTTGGAGAGGTTACTGGCGCGCCCTTCAATG-GAGAACC-3, respectively. The resulting mutant cDNA was digested with AscI and religated to obtain a PKD3 protein lacking amino acids 271–326. Point mutations to obtain catalytically inactive PKD3 were engineered using the forward (displayed) and complementary primers (not shown) PKD3/K605A, 5-GGGATGT-GGCTATTGCAGTGATTGATAAG-3 and PKD3/D720A, 5-GGT-GAAGCTGTGTGCCTTTGGATTTGCACGC-3. Vectors encoding fusion protein between a photoactivatable GFP (PAGFP) and wt PKD3, PKD3/K605A, or PKD3/D720A were obtained by isolating full-length PKD3 cDNAs from pGFP-PKD3, pGFP-PKD3/K605A, or pGFP-PKD3/D720A via KpnI digestion and subcloning the obtained DNAs into the KpnI site of pPAGFP-C1 (25). A plasmid encoding a fusion protein between PKD3 and a red fluorescent protein (RFP) was obtained by ligating a full-length PKD3 cDNA, isolated by KpnI digestion from pGFP-PKD3 (5), into the KpnI site of pDsRed-Express-C1 (Clontech). The vector encoding the fusion protein between PKD3/D720A and pFlag-CMV4 was obtained by isolating a BamHI cDNA fragment encompassing the D720A point mutations from pGFP-PKD3/D720A and exchanging this fragments for the equivalent one in pFlag-PKD3 (5, 23). All of the constructs were confirmed by DNA sequence analysis. A schematic representation of the proteins encoded by the different vectors used in this study, as well as their intracellular distribution, are depicted in Fig. 1*A*. Western blot analysis (5) was used to verify the size and stability of the chimeric proteins (Fig. 1*B*). Vectors encoding fusion proteins between GFP and wt PKD2 or wt PKD3, as well as FLAG-tagged wt PKD3, were previously described (5, 23). Earlier we demonstrated that the fusion of GFP or FLAG to the N terminus of the PKDs did not produce any detectable effect on their basal catalytic activity or GPCR agonists mediated activation (5, 17, 23).

Cell Culture, Transfections, Western Blots, in Vitro Kinase Assays, Exogenous Substrate Phosphorylation, and Immunoprecipitation—Panc-1 cells, Swiss 3T3 cells, HEK-293, and COS-7 cells were maintained and transfected or co-transfected (DNA ratio = 3/1 kinase dead PKD3/wt PKD3) as previously described (5, 11, 19, 22). Transfected cells were incubated for 18 h before live cell imaging, Western blot, or immunoprecipitation (19, 26). We used an antibody that specifically recognizes the phosphorylated state of Ser^{731}-Ser^{735} within the activation loop of PKD3 to determine its phosphorylation/activation state (5). Exogenous substrate syntide-2 phosphorylation by wt and mutant PKD3 proteins was assayed and quantified by Cerenkov counting as previously indicated (27). PKD3 autophosphorylation was determined by a kinase assay followed by SDS-PAGE analysis and quantification (27). Immunoprecipitations were performed as previously described (26).

Live Cell Imaging—To maintain a constant selected temperature during the experimental procedures, the cells were perfused with medium warmed to 37 °C, as described previously (5). The perfusion chamber was mounted on an epifluorescence microscope (Zeiss Axioskop, Carl Zeiss, Germany), and cell images were captured as uncompressed 24-bit TIFF files with a SPOT cooled (−12 °C) single CCD color digital camera (three pass method) driven by SPOT version 2.1 software (Diagnostic Instruments, Inc.) (5). GFP fluorescence was observed with a HI Q filter set for fluorescein isothiocyanate (Chroma Technology, VT). Additionally, the perfusion chamber was mounted in a laser scanning microscope PASCAL (Carl Zeiss, Germany), which had both 405 and 488 nm lasers, to photoactivate and image PAGFP-tagged proteins with a macro we developed to automate the photoconversion and measurement process. Applying this macro, we first obtained an image of a whole cell using excitation at 488 nm and emission at 500–560 nm (preactivation). Then the image was "zoomed" 40× to focus on a small area of the cell (7.0 μm × 7.0 μm) suitable for photoconversion. The region was then scanned for 1 s with the 405 nm laser to photoactivate the PAGFP-tagged protein within a predefined region. This was followed by a return to scanning mode at 488 nm, without the "zoom," at regular time intervals to track the movement of the photoactivated protein. Thirty cells were analyzed per experiment, and each experiment was performed at least three times. The selected cells displayed in the appropriate figures were representative of 80% of the population of PAGFP-positive cells.

Indirect Immunofluorescence—Indirect immunofluorescence was performed in 10% buffered formalin phosphate-fixed, 0.3% Triton X-100-PBS-permeabilized cultures. After extensive PBS washing, fixed cells were incubated for 18 h at 25 °C in blocking buffer (PBS, 1% gelatin, 0.05% Tween 20) (BB) and then stained at 25 °C for 60 min with a murine monoclonal antibody (M2) against the FLAG epitope. Subsequently, the cells were washed with PBS, 0.05% Tween 20 at 25 °C and stained at 25 °C for 60 min with Alexa Fluor 546-conjugated goat anti-mouse diluted in BB and washed again with PBS, 0.05% Tween 20. After a PBS and double-distilled water wash, the samples were mounted with a gelvatol-glycerol solution containing 2.5% 1,4-diazobicyclo-[2,2,2]octane (19). The samples were examined and imaged with an epifluorescence microscope and a Zeiss oil immersion objective (Plan-Apochromat 40×/1.0, Carl Zeiss Inc.). Images were captured as described above. Fluorescein or Alexa Fluor 546 signals were observed with HI Q filter sets for fluorescein isothiocyanate or rhodamine/TRITC, respectively (Chroma Technology). The selected cells displayed in the appropriate figures were representative of 80% of the population of positive cells.

Materials—[γ-^{32}P]ATP (370 MBq/ml), horseradish peroxidase-conjugated donkey anti-rabbit and anti-mouse IgG were from Amersham Biosciences. Alexa Fluor 546 goat anti-mouse antibody was obtained from Molecular Probes. Primary antibodies were obtained from: Cell

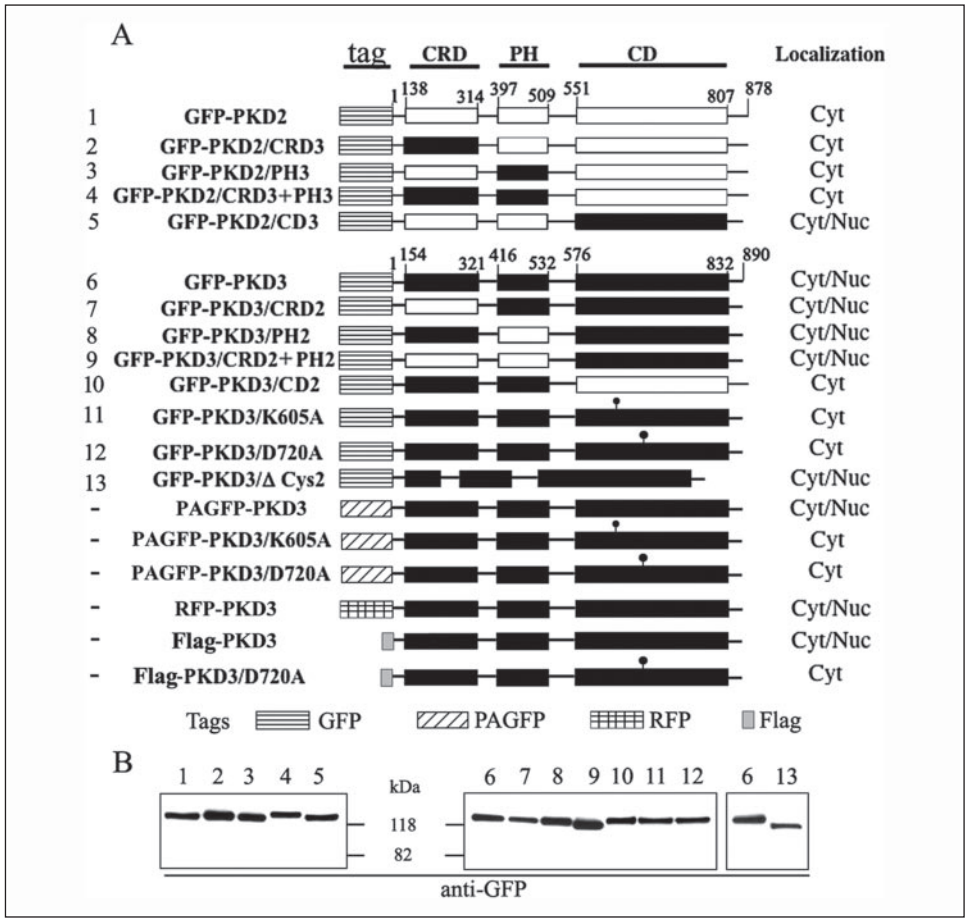

FIGURE 1. **Schematic representation, intracellular localization, and Western blot analysis of the expressed PKD2/PKD3 chimeras and PKD3 mutant proteins.** *A,* numbers correspond to amino acid residue position. *Cyt*, cytosol; *Nuc*, nucleus; *Cd*, catalytic domain. *B*, total cell lysates obtained from Panc-1 cells transiently transfected with plasmids encoding the proteins indicated by the numbers on the left column of *A* were analyzed by SDS 4–15% PAGE and Western blot using a murine monoclonal antibody against GFP.

Signaling Technology (anti-loop phospho-PKD/PKCμ Ser^{744}-Ser^{748}, which recognizes the phosphorylation status of PKD, PKD2, and PKD3 activation loop), Sigma (anti-Flag M2), and BD Biosciences (anti-importin β, anti-importin α, and anti-GFP). All of the other reagents were the highest grade commercially available.

RESULTS AND DISCUSSION

Role of the N-terminal Region of PKD3 in Its Nuclear Localization—Although PKD2 and PKD3 share extensive structural homology (10), they localize in different cellular compartments, *i.e.* PKD2 is predominantly in the cytoplasm, whereas PKD3 is found both in the cytoplasm and nucleus of unstimulated fibroblast and epithelial cells (5, 23). To identify the domain(s) of PKD3 that mediates its constitutive nuclear localization, we generated a set of chimeras between both isozymes (Fig. 1*A*) and examined the distribution of the resulting GFP-tagged proteins by live cell imaging.

Because the CRD and PH domains of PKD play an important role in determining its intracellular localization (19, 20), we replaced the CRD or PH domain of PKD2 with the CRD or PH domain from PKD3, and examined the cellular distribution of the resulting proteins. Panc-1 cells, a human pancreatic cell line that expresses all known PKD isoforms (5, 23, 28), were transiently transfected with pGFP-PKD2/CRD3 or pGFP-PKD2/PH3 and examined 18 h post-transfection. As Fig. 2*A* shows, neither the CRD nor the PH domain of PKD3 induce redistribution from the cytosol into the nucleus of GFP-PKD2/CRD3 or GFP-PKD2/PH3, indicating that these domains are not sufficient to promote the nuclear localization of these chimeric proteins. To further substantiate this conclusion, we replaced the CRD and PH domain of PKD3 by the equivalent domains isolated from PKD2. The resulting chimeras, GFP-PKD3/CRD2 and GFP-PKD3/PH2, showed a cytosolic and nuclear localization indistinguishable from wt PKD3 (Fig. 2*B*), indicating that neither the CRD nor the PH domain of PKD2 prevented the nuclear localization of PKD3.

Further support for this conclusion was obtained by simultaneously replacing the CRD and PH domains of PKD2 for their PKD3 equivalents. The resulting fusion protein, GFP-PKD2/CRD3+PH3, displayed the same intracellular distribution as wt PKD2, *i.e.* it was present in the cytosol and excluded from the nucleus (Fig. 2*A*). Reciprocally, a chimera containing the CRD and PH domain of PKD2 and the C-terminal kinase region of PKD3 (GFP-PKD3/CRD2+PH2) had the same intracellular distribution as wt PKD3 (Fig. 2*B*), indicating that the N-terminal region of PKD3 is not sufficient to promote its nuclear localization.

A classical nuclear localization signal has not been documented in PKD. However, its nuclear accumulation in response to GPCR stimulation can be completely prevented by deleting its cys2 domain (20). Consequently, we deleted the cys2 domain of PKD3 and transiently expressed the mutated protein in Panc-1 cells. As shown in Fig. 2*C*, the deletion of the cys2 of PKD3 caused a conspicuous reduction in GFP-PKD3/Δcys2 nuclear localization. However, this deletion did not block the nuclear entry of PKD3 to the extent observed with PKD/Δcys2 (20), supporting the conclusion that another domain of PKD3 outside its N-terminal region is involved in its nuclear localization.

PKD3 Nuclear Localization Requires Its Catalytic Activity—In view of the preceding results, we exchanged the C-terminal regions of PKD2 and PKD3 (Fig. 1*A*) and examined the intracellular distribution of GFP-PKD2/CD3 and GFP-PKD3/CD2 in live cells. Surprisingly, we found that the intracellular distribution of GFP-PKD2/CD3 was indistinguishable from GFP-PKD3 (Fig. 3*A*), indicating that the replacement of the

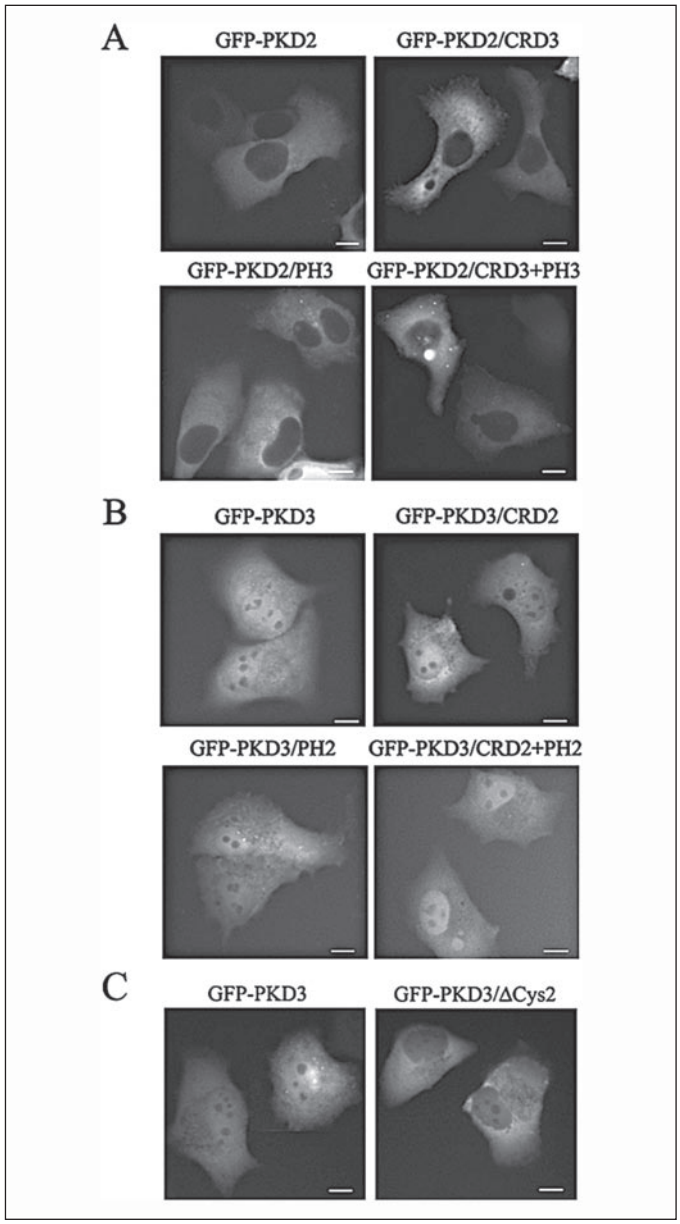

FIGURE 2. **Intracellular distribution of PKD2/PKD3 chimeras corresponding to their N-terminal regulatory region.** Panc-1 cells were transiently transfected with plasmids encoding the indicated proteins and incubated at 37 °C for 18 h. An epifluorescence microscope was used to visualize the distribution of the GFP-tagged proteins in living cells. Representative images were captured as described under "Experimental Procedures." The selected cells displayed in the figures were representative of 80% of the population of positive cells. *Bar*, 10 μm.

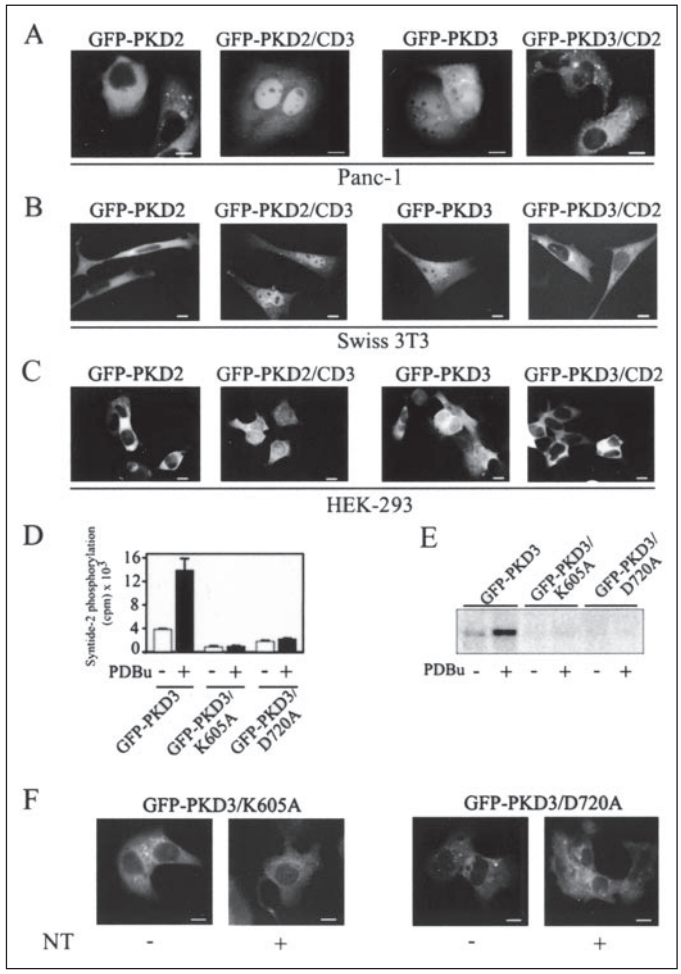

FIGURE 3. **Intracellular distribution of PKD2/PKD3 chimeras and mutant proteins corresponding to their C-terminal kinase region.** Panc-1 (*A*), Swiss 3T3 (*B*), and HEK-293 cells (*C*) were transiently transfected with plasmids encoding the indicated proteins and incubated at 37 °C for 18 h. An epifluorescence microscope was used to visualize the distribution of the GFP-tagged proteins in live cells. COS-7 cells transiently transfected with plasmids encoding the indicated proteins were stimulated for 10 min with 200 nM PDBu and lysed, and the catalytic activity of wt and mutant PKD3 proteins assayed by syntide-2 phosphorylation (*D*) and *in vitro* kinase assay (*E*) as described under "Experimental Procedures." Panc-1 cells transiently transfected with plasmids encoding GFP-PKD3/K605A or GFP-PKD3/D720A were examined 18 h post-transfection with an epifluorescence microscope to visualize the distribution of the GFP-tagged proteins in live cells before or after 10 min NT (50 nM) stimulation (*F*). Representative images were captured as described under "Experimental Procedures." The selected cells displayed in the figures were representative of 80% of the population of positive cells. *Bar*, 10 μm.

C-terminal region of PKD2 by the equivalent region from PKD3 was sufficient to promote the nuclear localization of this chimeric protein. Conversely, the substitution of the C-terminal region of PKD3 for the equivalent domain of PKD2 resulted in a chimeric protein that had the same distribution as wt PKD2 (Fig. 3*A*). Similar results were obtained when GFP-PKD2/CD3 and GFP-PKD3/CD2 were expressed in Swiss 3T3 fibroblasts (Fig. 3*B*), HEK-293 (Fig. 3*C*), and COS-7 cells (data not shown), demonstrating that the nuclear localization mediated by the C-terminal kinase region of PKD3 is not restricted to Panc-1 cells.

The results presented above showing that the C-terminal kinase region of PKD3 was necessary for its nuclear localization prompted us to investigate whether its catalytic activity was also required because the intracellular distribution of several kinases is associated to their catalytic activity (29–31). We engineered two different kinase-defective PKD3 mutant proteins to address this issue. In the first mutant, the lysine 605 at the ATP binding site was substituted with alanine (PKD3/K605A), while in the second one the highly conserved aspartic acid located at position 720 in the DFG motif, which is critical for kinase catalytic activity (32), was mutated to alanine (PKD3/D720A).

To verify the properties of these mutants, COS-7 cells expressing GFP-PKD3, GFP-PKD3/K605A, or GFP-PKD3/D720A were stimulated with phorbol 12,13-dibutyrate (PDBu) for 10 min and lysed, and the fusion proteins were immunoprecipitated from the extracts with an antibody against GFP. PKD3 activity in the immunocomplexes was determined by phosphorylation of syntide-2, an excellent substrate for PKD3 (5). In agreement with our previous results, GFP-PKD3 isolated from unstimulated cells had low catalytic activity that was markedly activated by PDBu stimulation of intact cells (Fig. 3*D*). In contrast, no kinase activity was associated with the immunoprecipitated GFP-PKD3/K605A or GFP-PKD3/D720A proteins before and after PDBu

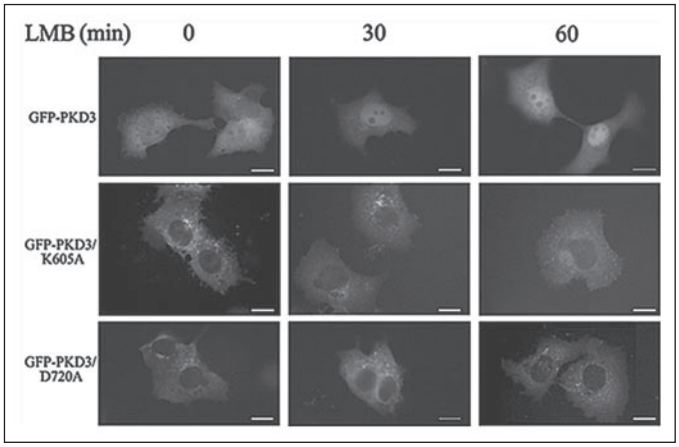

FIGURE 4. **Effect of CRM1-dependent nuclear export inhibition in the intracellular distribution of PKD3.** Panc-1 cells were transfected with plasmids encoding the indicated proteins and incubated at 37 °C for 18 h. Cultures were untreated or treated with LMB (10 ng/ml) during the indicated times. An epifluorescence microscope was used to visualize the distribution of the GFP-tagged proteins in living cells. Representative images were captured as described under "Experimental Procedures." The selected cells displayed in the figures were representative of 80% of the population of positive cells. *Bar*, 10 μm.

stimulation (Fig. 3*D*). Similar results were obtained when PKD3 activity in the immunocomplexes was determined by PKD3 autophosphorylation (Fig. 3*E*).

Once we established that GFP-PKD3/K605A and GFP-PKD3/D720A were catalytically inactive, these proteins were expressed in Panc-1 cells, and their intracellular distribution was examined in live cells 18 h post-transfection. In contrast to the nuclear and cytoplasmic localization of GFP-PKD3, GFP-PKD3/K605A and PKD3/D720A were present predominantly in the cytoplasm of Panc-1, even after GPCR stimulation (Fig. 3*F*). Thus, these results demonstrated that the nuclear localization of PKD3 requires its catalytic activity. These findings are not restricted to Panc-1 cells because similar results were obtained with COS-7 cells (data not shown).

PKD3 Nuclear Import Requires Its Catalytic Activity—Having established that the nuclear localization of PKD3 requires its catalytic activity, we examined whether the cytoplasmic localization of catalytically inactive PKD3 was due to a faster rate of nuclear export than import. We previously demonstrated that leptomycin B (LMB), an antifungal antibiotic that inhibits the CRM1-dependent nuclear export pathway (33–35), blocks the nuclear export of PKD3 (5). Consequently, Panc-1 cells transiently transfected with plasmids encoding wt or catalytically inactive PKD3 proteins were incubated with LMB (10 ng/ml), and the distribution of GFP-tagged proteins was analyzed by imaging live cells. As shown in Fig. 4, the nuclear localization of wt PKD3 was rapidly enhanced by LMB treatment. In contrast, LMB treatment did not induce any nuclear accumulation of the catalytically inactive PKD3/K605A or PKD3/D720A mutant proteins even after 60 min of treatment (Fig. 4). Thus, the cytoplasmic localization of these inactive kinases was due to impaired nuclear import rather than faster rate of nuclear export.

Intra- and Intercompartmental Dynamics of wt and Catalytically Inactive PKD3—To gain a better understanding of the dynamic behavior of PKD3 and to further support the conclusion that the catalytic activity of PKD3 is required for its nuclear import, we generated plasmids encoding wt or catalytically inactive PKD3 mutant proteins fused to PAGFP (25). Photoactivation of PAGFP-tagged proteins is a recently developed methodology for examining the mobility and compartmental residence of a small population of molecules with high spatial and temporal resolution (36–38). Panc-1 cells transiently transfected with plasmids encoding PAGFP-PKD3, PAGFP-PKD3/K605A, or PAGFP-PKD3/D720A were incubated for 18 h at 37 °C before photoactivation and imaging as indicated under "Experimental Procedures." Photoactivation was performed either in the cytoplasmic or nuclear compartments, within the restricted areas indicated by a white rectangle (Fig. 5). After photoactivation, the total cell fluorescence was followed over time.

As illustrated by the images presented in Fig. 5, *top panels*, a very strong fluorescence was observed within 8 s after nuclear PAGFP-PKD3 photoactivation. The very rapid nuclear equilibration of photoactivated PAGFP-PKD3 coincided with its nuclear export, which was evident in the appearance of fluorescence in the cytoplasm 28 s after photoactivation. The subsequent equilibration of the fluorescent signal throughout the cell was concomitant with a drop in the intensity of the nuclear signal, indicating further transfer of PAGFP-PKD3 from that compartment into the cytoplasm.

The photoactivation of cytoplasmic PAGFP-PKD3 also revealed an extremely rapid movement of the fluorescent signal from the point of photoactivation to the surrounding cytoplasm (Fig. 5, *middle panels*). This rapid movement was followed by an increase in the nuclear fluorescence within 63 s of photoactivation and a decrease in the intensity of the cytoplasmic fluorescent signal, demonstrating that in non-stimulated Panc-1 cells PKD3 continuously shuttles between the cytoplasm and nucleus.

The photoactivation of cytoplasmic PAGFP-PKD3/K605A also revealed the movement of the fluorescent signal from the point of photoactivation to the surrounding cytoplasm as occurred with PAGFP-PKD3 (Fig. 5). However, PAGFP-PKD3/K605A did not enter the nucleus. Interestingly, we observed that the rate of PAGFP-PKD3/K605A movement in the cytoplasm was slower than PAGFP-PKD3, suggesting that this mutant was interacting with another protein or cellular component that impaired its rapid diffusion.

To confirm these results, we also examined the dynamic distribution of the PAGFP-PKD3/D720A in Panc-1 cells. As occurred with PAGFP-PKD3/K605A, PAGFP-PKD3/D720A remained in the cytoplasm even 4.5 min after photoactivation, and its cytoplasmic movement was slower than PAGFP-PKD3, further indicating that PKD3 catalytic activity is associated to its nuclear import and rapid intracellular movement. No fluorescence was detected in cells expressing PAGFP-PKD3/K605A or PAGFP-PKD3/D720A after nuclear photoactivation (data not shown).

Collectively, these results demonstrated that the nuclear import of PKD3 requires its catalytic activity and that wt PKD3 is continuously shuttling between both compartments. In addition, these results show that wt PKD3 moves rapidly within the nucleus and cytoplasm, advancing the novel concept that PKD3 is freely diffusible within these compartments.

PKD3 Interacts with Importins β and α Independently of Its Catalytic Activity—The transport of ions, small molecules, and proteins between the cytoplasm and nucleus occurs by passive diffusion through the nuclear pore complex, a large cylindrical structure spanning the nuclear envelope (39). However, the interchange of large macromolecules through the nuclear pore complex occurs by an active process involving several adaptor proteins called importins and exportins (39). Importin β, the first carrier to be identified, mediates the import of proteins through another adaptor protein called importin α. In addition, importin β can directly interact with some cargoes to mediate their nuclear import independently of importin α (40). Because the results presented in Fig. 4 demonstrate that the cytosolic localization of inactive PKD3

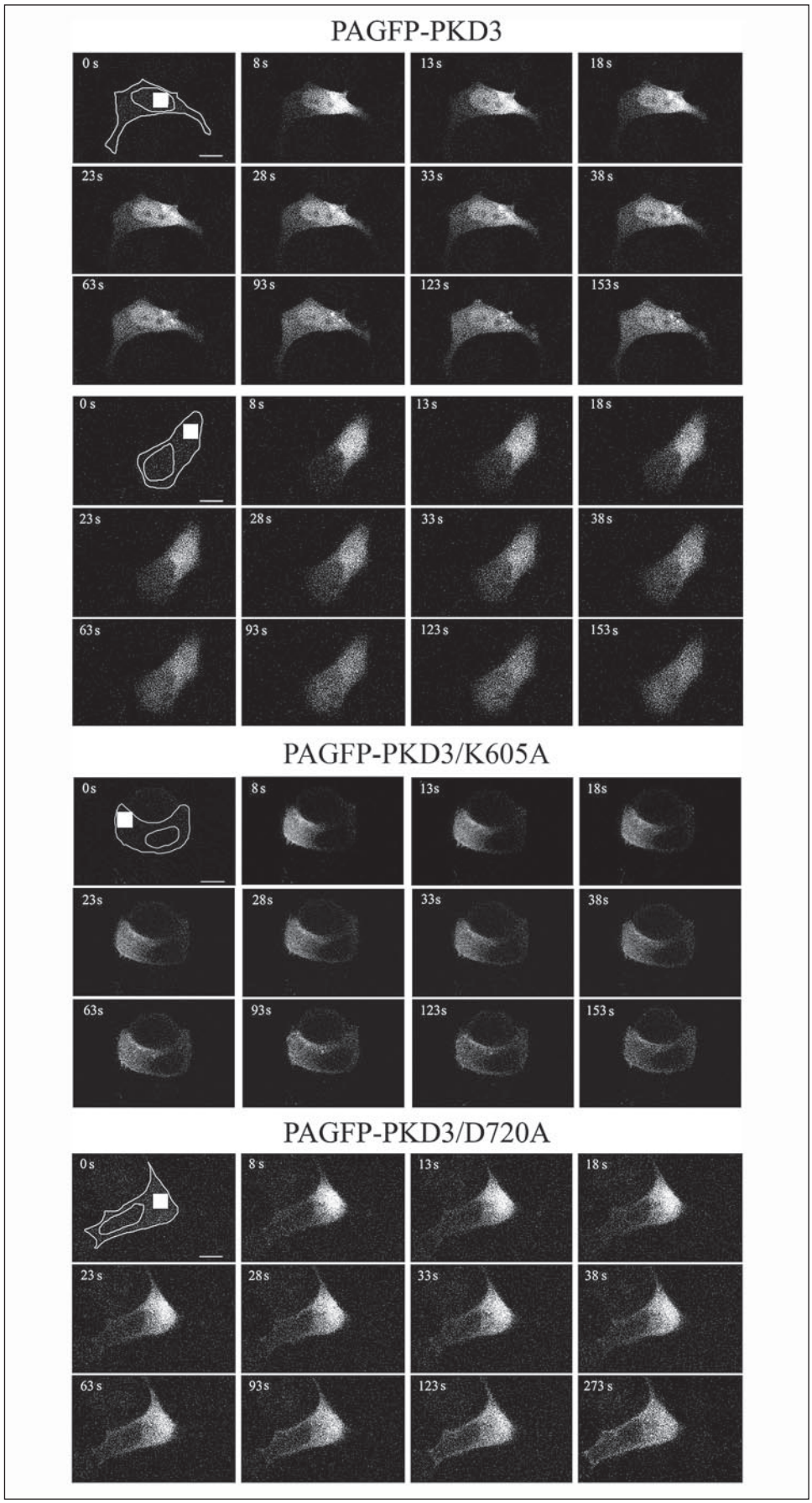

FIGURE 5. **Intra- and intercompartmental dynamics of wt and catalytically inactive PKD3.** Panc-1 cells were transfected with plasmids encoding a fusion protein between wt or the catalytically inactive PKD3/K605A or PKD3/D720A proteins and a PAGFP and examined 18 h post-transfection using a LSM as described under "Experimental Procedures." Photoactivation was performed in the cytoplasm or nuclear compartment within the area indicated by a *white rectangle*. The selected cells displayed in the figures were representative of 80% of the population of positive cells. *Bar*, 10 μm.

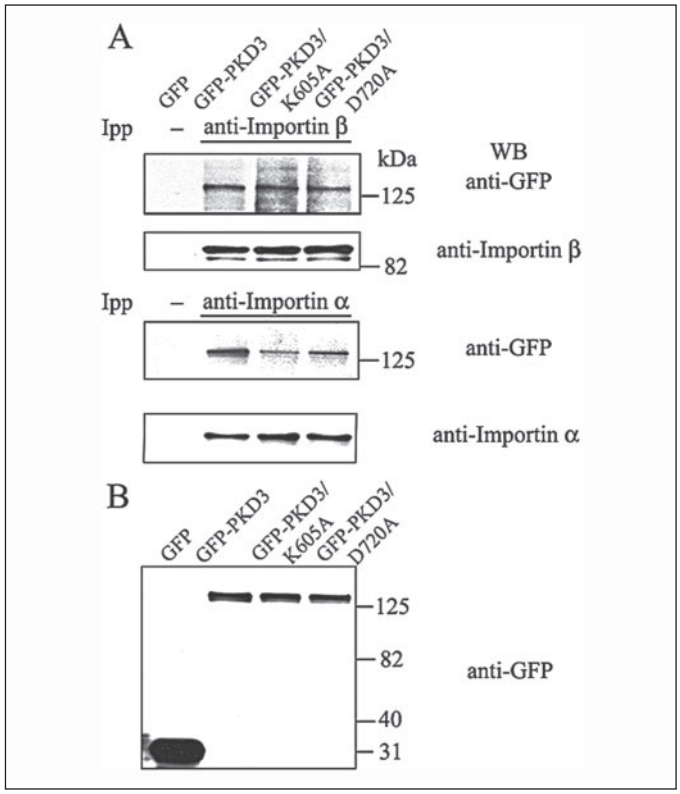

FIGURE 6. **Determination of PKD3 binding toward importin β and α.** *A*, Panc-1 cells transiently transfected with plasmids encoding GFP, GFP-tagged wt, or catalytically inactive PKD3 proteins were incubated 18 h before lysis. The lysates were incubated with Protein A/G-agarose (−) or immunoprecipitated (*Ipp*) with the indicated antibodies and the immunocomplexes extracted with gel loading buffer and analyzed by SDS 4–15% PAGE followed by Western blot analysis (*WB*) using antibodies against GFP, importin β, or importin α. Results are representative of three independent experiments. *B*, total cell lysates used for immunoprecipitation were analyzed by SDS 4–15% PAGE and Western blot using a murine monoclonal antibody against GFP.

was because of a defect in its nuclear import, we examined whether catalytically inactive PKD3 was able to interact with importins β and α.

Lysates obtained from Panc-1 cultures transiently transfected with pEGFP-C1 (empty vector), pGFP-PKD3, pGFP-PKD3/K605A, or pGFP-PKD3/D720A were immunoprecipitated with antibodies against importin β or α and the immune complexes analyzed by SDS-PAGE and Western blot. As seen in Fig. 6*A*, wt or catalytically inactive GFP-tagged PKD3 mutants were present in the complexes obtained with the anti-importin β or α antibodies, indicating that the interaction between PKD3 and these importins is not sufficient to mediate its nuclear import. Interestingly, more wt PKD3 than catalytically inactive PKD3 proteins co-immunoprecipitated with importin α, suggesting that wt PKD3 interacts more efficiently with this importin. Although a nuclear localization signal has not been identified to date in PKD3, several motifs resembling classical nuclear localization signal are present in its C-terminal region raising the possibility that the interaction between importins and PKD3 is mediated by one of these motifs. Western blot analysis of the cell lysates used for the immunoprecipitations shown that GFP-tagged wt and kinase dead PKD3 proteins were expressed at similar levels (Fig. 6*B*).

The Activation Loop Phosphorylation of PKD3 Does Not Require Its Nuclear Localization and Is Not Sufficient to Promote Its Nuclear Import—One of the functional characteristics of nuclear transport receptors is the saturability of signal recognition (41). We used this criterion to determine whether the catalytically inactive PKD3/K605A and PKD3/D720A proteins were able to block the nuclear import of wt PKD3. Panc-1 cells were co-transfected with pRFP-PKD3 and pGFP-PKD3/K605A or pGFP-PKD3/D720, and the intracellular distribution of the encoded proteins was examined in live cells 18 h post-transfection. In agreement with the results obtained with GFP-tagged wt PKD3, RFP-tagged wt PKD3 was distributed throughout the cytosol and the nuclei of Panc-1 cells. However, catalytically inactive PKD3 proteins prevented the nuclear import of wt PKD3 (Fig. 7*A*). Co-expression of GFP, which is uniformly distributed in the cytoplasm and nuclei of Panc-1 cells, did not interfere with the nuclear localization of RFP-PKD3 (data not shown). These results indicated that catalytically inactive PKD3 successfully competed with wt PKD3 for the nuclear import receptor in charge of delivering PKD3 to the nucleus.

A sequential model of activation and intracellular distribution of the PKDs in response to DAG production has been recently proposed (10). Within this model, the activation loop phosphorylation of PKD3 plays a critical role in the early steps of its dynamic response to DAG production, *i.e.* rapid plasma membrane dissociation. However, no previous studies examined whether PKD3 activation loop phosphorylation occurs in the cytoplasm or its role in the nuclear transport of PKD3.

Having established that the nuclear import of wt PKD3 is blocked by co-expression of catalytically inactive PKD3 proteins, we used this system to determine whether PKD3 activation loop phosphorylation requires its nuclear localization and to dissect its role in the nuclear import of PKD3. Catalytically active and inactive PKD3 proteins were tagged either with the FLAG epitope or with GFP, respectively, to distinguish them by differential migration in SDS-PAGE. Panc-1 cells transiently co-transfected with plasmids encoding FLAG-tagged wt PKD3 and GFP or GFP-PKD3 (wt) or GFP-PKD3/D720A were challenged for 10 min with PDBu or the GPCR agonist neurotensin (NT) and lysed. The solubilized proteins were resolved by SDS-PAGE and examined by Western blot using an antibody that recognizes the phosphorylated state of Ser^{731} and Ser^{735} within the activation loop of PKD3.

PDBu or NT promoted the phosphorylation of the activation loop of wt PKD3 expressed alone or with the catalytically inactive PKD3 proteins (Fig. 7*B*). Interestingly, PDBu or NT also induced the activation loop phosphorylation of the catalytically inactive PKD3 proteins (Fig. 7*B*), demonstrating that PKD3 kinase activity is not required to catalyze its activation loop phosphorylation and further reinforcing the concept that PKDs activation loop phosphorylation occurs by transphosphorylation (10). In addition, and because the nuclear import of wt PKD3 was inhibited by catalytically inactive PKD3 (Fig. 7*A*), the results presented in Fig. 7*B* also indicated that PKD3 activation loop phosphorylation does not require its nuclear localization. The same membranes were stripped and subsequently probed with a mix of anti-FLAG and anti-GFP antibodies (Fig. 7*B*) to verify the expression and gel loading of the different proteins. Similar results were obtained when the cells were challenged for 10 min with either 5 or 25 nM NT (data not shown).

To further confirm that catalytically inactive PKD3 inhibited the nuclear import of wt PKD3, Panc-1 cells were transfected with FLAG-tagged wt PKD3 and GFP or GFP-PKD3 (wt) or GFP-PKD3/D720, and their intracellular distribution was examined by immunocytochemistry. As shown in Fig. 7*C*, *top panels*, Flag-PKD3 was distributed throughout the cytosol and the nuclei of Panc-1 cells when expressed with GFP or GFP-PKD3 (Fig. 7*C*), demonstrating that the nuclear localization of these proteins did not prevent the nuclear entry of Flag-PKD3. However, and in agreement with the results presented in Fig. 7*A*, the nuclear localization of Flag-PKD3 was prevented by the co-expression of GFP-PKD3/D720A. GPCR stimulation did not modify the distribution of Flag-PKD3 co-expressed with GFP, GFP-PKD3, or with GFP-PKD3/

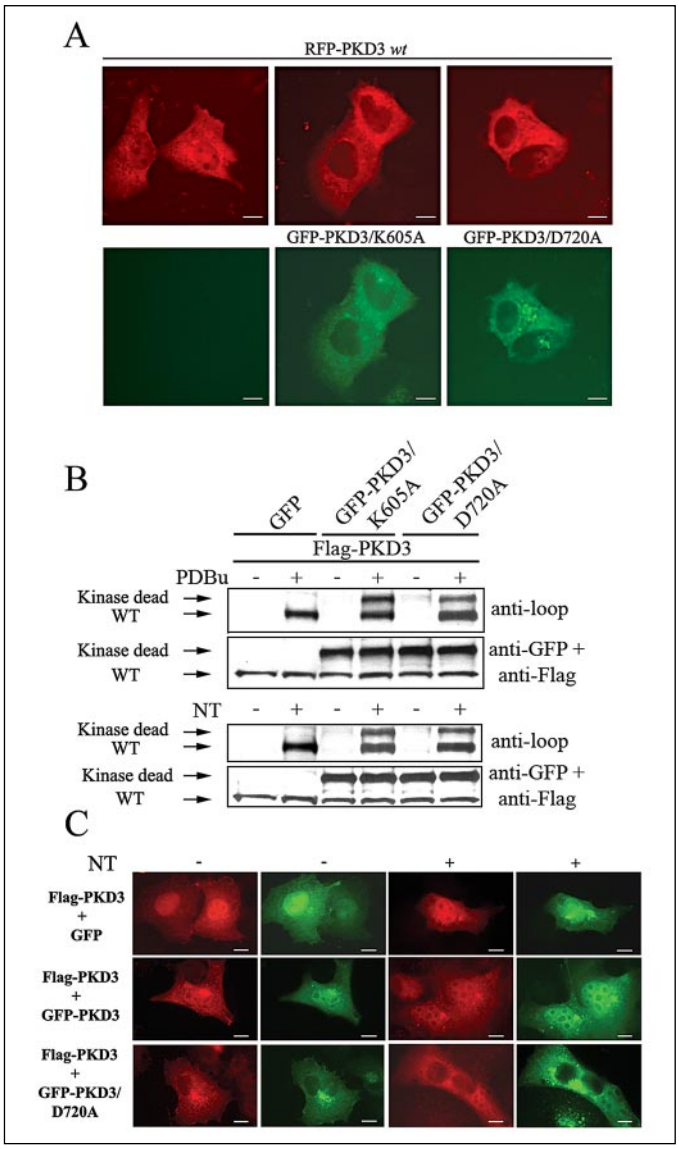

FIGURE 7. **Intracellular distribution of wt PKD3 in the presence of catalytically inactive PKD3 mutants in live cells.** *A*, Panc-1 cells were transiently co-transfected with plasmids encoding RFP-tagged wt PKD3 and GFP-tagged mutants PKD3/K605A or PKD3/D720A and incubated at 37 °C for 18 h. An epifluorescence microscope was used to visualize the distribution of the GFP- and RFP-tagged proteins in living cells. Representative images were captured as described under "Experimental Procedures." The selected cells displayed in the figures were representative of 80% of the population of positive cells. *Bar*, 10 μm. *B*, activation loop phosphorylation status of co-expressed wt and catalytically inactive PKD3 proteins. Panc-1 cells transiently transfected with pFlag-PKD3 and pEGFP-C1 (empty vector), GFP-PKD3/K605A, or GFP-PKD3/D720A were stimulated 18 h post-transfection with 200 nM PDBu or 50 nM NT for 10 min and lysed, and the lysates were resolved by SDS 4–15% PAGE followed by Western blot analysis using antibodies that detect the phosphorylation status of PKD3 activation loop (*anti-loop*) or antibodies directed against GFP and FLAG. Results are representative of three independent experiments. *C*, intracellular distribution of wt PKD3 in the presence of catalytically inactive PKD3 mutants in fixed cells. Panc-1 cells were transiently cotransfected with plasmids encoding FLAG-tagged wt PKD3 and GFP or GFP-PKD3 or GFP-PKD3/D720A and incubated at 37 °C for 18 h. Cells were stimulated (+) or not (−) with 50 nM NT for 10 min and processed for immunocytochemistry as described under "Experimental Procedures" using a murine monoclonal antibody against FLAG followed by Alexa Fluor 546 goat anti-mouse antibody. An epifluorescence microscope was used to examine the distribution of GFP-and FLAG-tagged proteins. Representative images were captured as described under "Experimental Procedures." The selected cells displayed in the figures were representative of 80% of the population of positive cells. *Bar*, 10 μm.

D720A. These results, together with those presented in Fig. 7*B*, demonstrated that the phosphorylation of the activation loop of PKD3 does not require its nuclear localization and that it is not sufficient to promote the nuclear entry of PKD3.

Concluding Remarks—Increasing experimental evidence supports the notion that the targeting of signaling molecules to different cellular compartments is a fundamental process in the regulation of their function (13–15). In recent years, an increasing number of regulatory protein kinases including PKCλ, Bruton's tyrosine kinase, Abl, and mitogen-activated protein kinase (MAPK/ERK), have been shown to shuttle between the nucleus and the cytoplasm (13–15, 30, 42–47). In the present study, we used visualization of GFP-tagged PKD2/PKD3 chimeras and photoactivatable-tagged PKD3 mutant proteins to define the molecular determinants that mediate the nuclear import of PKD3.

A salient feature of the results presented here, which are summarized in Fig. 1*A*, is that the catalytic activity of PKD3 is required to promote its nuclear import. Three different lines of evidence support this conclusion. First, we observed that the exchange of the C-terminal regions of PKD2 and PKD3, but not their N-terminal regulatory regions, was sufficient to exchange their intracellular localization. Second, inhibition of the LMB-sensitive CRM1-nuclear export pathway employed by PKD3 (5) did not induce nuclear accumulation of the catalytically inactive PKD3/K605A or PKD3/D720A mutant proteins. Third, real time imaging of fusion proteins between a photoactivatable GFP and wt or PKD3 mutant proteins demonstrated that the catalytically inactive PKD3 proteins were excluded from the nucleus.

Interestingly, we also found that the deletion of the cys2 domain of PKD3 reduced, but did not block, its nuclear localization to the extent observed when an equivalent deletion was introduced in PKD (20) implying that the nuclear localization of PKD3, and probably the transient nuclear localization of other PKDs, is governed by its multiple domains acting sequentially. Considering that PKDs are able to interact with different proteins (10) and that the rate of cytoplasmic diffusion of catalytically inactive PKD3 is reduced, it is tempting to speculate that the catalytic activity is required to promote, or alternatively remove, a protein(s) that regulates the nuclear transport of PKD3.

Recently, a sequential model of activation that integrates the spatial and temporal changes of the PKDs has been proposed (10). Within the framework of this model, the steady-state distribution of PKD3 results from a nucleocytoplasmic shuttling in which the rate of nuclear import exceeds that of nuclear export. The production of DAG at the plasma membrane, *e.g.* in response to GPCR stimulation, promotes the translocation of PKD3 from the cytosol to the plasma membrane where novel PKCs are also recruited in response to DAG generation. Novel PKCs, allosterically activated by DAG, transphosphorylate PKD3 at Ser^{731} and Ser^{735}. This event stabilizes the activation loop of this enzyme in an active conformation, induces its rapid plasma membrane dissociation, and further promotes its nuclear accumulation. The results presented here are of special relevance for this model because they 1) identify a novel requirement regulating the dynamic distribution of PKD3 and very likely the other PKD isozymes, *i.e.* catalytic activity, 2) provide evidence that the activation loop phosphorylation of PKD3 occurs in the cytoplasm, 3) show that PKD3 interacts with importin α and β and that this interaction is not sufficient to promote its nuclear localization, and 4) demonstrate that activation loop phosphorylation is not sufficient to promote the nuclear import of PKD3.

In conclusion, the results presented in this study identify a critical and novel function for the kinase activity of PKD3 in promoting its nuclear entry and suggest that its catalytic activity may regulate PKD3 nuclear import through autophosphorylation and/or interaction with another protein(s).

Acknowledgments—We are very grateful to Dr. M. Yoshida, from the Department of Biotechnology, University of Tokyo, for the generous gift of Leptomycin B.

REFERENCES

1. Valverde, A. M., Sinnett-Smith, J., Van Lint, J., and Rozengurt, E. (1994) *Proc. Natl. Acad. Sci. U. S. A.* **91,** 8572–8576
2. Johannes, F. J., Prestle, J., Eis, S., Oberhagemann, P., and Pfizenmaier, K. (1994) *J. Biol. Chem.* **269,** 6140–6148
3. Hayashi, A., Seki, N., Hattori, A., Kozuma, S., and Saito, T. (1999) *Biochim. Biophys. Acta* **1450,** 99–106
4. Sturany, S., Van Lint, J., Muller, F., Wilda, M., Hameister, H., Hocker, M., Brey, A., Gern, U., Vandenheede, J., Gress, T., Adler, G., and Seufferlein, T. (2001) *J. Biol. Chem.* **276,** 3310–3318
5. Rey, O., Yuan, J., Young, S. H., and Rozengurt, E. (2003) *J. Biol. Chem.* **278,** 23773–23785
6. Rozengurt, E., Sinnett-Smith, J., and Zugaza, J. L. (1997) *Biochem. Soc. Trans.* **25,** 565–571
7. Iglesias, T., Matthews, S., and Rozengurt, E. (1998) *FEBS Lett.* **437,** 19–23
8. Iglesias, T., and Rozengurt, E. (1998) *J. Biol. Chem.* **273,** 410–416
9. Iglesias, T., and Rozengurt, E. (1999) *FEBS Lett.* **454,** 53–56
10. Rozengurt, E., Rey, O., and Waldron, R. T. (2005) *J. Biol. Chem.* **280,** 13205–13208
11. Waldron, R. T., Rey, O., Iglesias, T., Tugal, T., Cantrell, D., and Rozengurt, E. (2001) *J. Biol. Chem.* **276,** 32606–32615
12. Sturany, S., Van Lint, J., Gilchrist, A., Vandenheede, J. R., Adler, G., and Seufferlein, T. (2002) *J. Biol. Chem.* **277,** 29431–29436
13. Jaken, S. (1996) *Curr. Opin. Cell Biol.* **8,** 168–173
14. Newton, A. C. (1997) *Curr. Opin. Cell Biol.* **9,** 161–167
15. Teruel, M. N., and Meyer, T. (2000) *Cell* **103,** 181–184
16. Prestle, J., Pfizenmaier, K., Brenner, J., and Johannes, F. J. (1996) *J. Cell Biol.* **134,** 1401–1410
17. Matthews, S., Iglesias, T., Cantrell, D., and Rozengurt, E. (1999) *FEBS Lett.* **457,** 515–521
18. Storz, P., Hausser, A., Link, G., Dedio, J., Ghebrehiwet, B., Pfizenmaier, K., and Johannes, F. J. (2000) *J. Biol. Chem.* **275,** 24601–24607
19. Rey, O., Young, S. H., Cantrell, D., and Rozengurt, E. (2001) *J. Biol. Chem.* **276,** 32616–32626
20. Rey, O., Sinnett-Smith, J., Zhukova, E., and Rozengurt, E. (2001) *J. Biol. Chem.* **276,** 49228–49235
21. Rey, O., Zhukova, E., Sinnett-Smith, J., and Rozengurt, E. (2003) *J. Cell. Physiol.* **196,** 483–492
22. Rey, O., Young, S. H., Yuan, J., Slice, L., and Rozengurt, E. (2005) *J. Biol. Chem.* **280,** 22875–22882
23. Rey, O., Yuan, J., and Rozengurt, E. (2003) *Biochem. Biophys. Res. Commun.* **302,** 817–824
24. Rey, O., Reeve, J. R., Jr., Zhukova, E., Sinnett-Smith, J., and Rozengurt, E. (2004) *J. Biol. Chem.* **279,** 34361–34372
25. Patterson, G. H., and Lippincott-Schwartz, J. (2002) *Science* **297,** 1873–1877
26. Jacamo, R., Lopez, N., Wilda, M., and Franze-Fernandez, M. T. (2003) *J. Virol.* **77,** 10383–10393
27. Waldron, R. T., Iglesias, T., and Rozengurt, E. (1999) *J. Biol. Chem.* **274,** 9224–9230
28. Guha, S., Rey, O., and Rozengurt, E. (2002) *Cancer Res.* **62,** 1632–1640
29. Lemrow, S. M., Anderson, K. A., Joseph, J. D., Ribar, T. J., Noeldner, P. K., and Means, A. R. (2004) *J. Biol. Chem.* **279,** 11664–11671
30. Mohamed, A. J., Vargas, L., Nore, B. F., Backesjo, C. M., Christensson, B., and Smith, C. I. (2000) *J. Biol. Chem.* **275,** 40614–40619
31. Lee, K. K., and Yonehara, S. (2002) *J. Biol. Chem.* **277,** 12351–12358
32. Hanks, S. K., and Hunter, T. (1995) *FASEB J.* **9,** 576–596
33. Fornerod, M., Ohno, M., Yoshida, M., and Mattaj, I. W. (1997) *Cell* **90,** 1051–1060
34. Ossareh-Nazari, B., Bachelerie, F., and Dargemont, C. (1997) *Science* **278,** 141–144
35. Wolff, B., Sanglier, J. J., and Wang, Y. (1997) *Chem. Biol.* **4,** 139–147
36. Lippincott-Schwartz, J., Altan-Bonnet, N., and Patterson, G. H. (2003) *Nat. Cell Biol.* **Suppl**, 7–14
37. Lippincott-Schwartz, J., and Patterson, G. H. (2003) *Science* **300,** 87–91
38. Patterson, G. H., and Lippincott-Schwartz, J. (2004) *Methods* **32,** 445–450
39. Chook, Y. M., and Blobel, G. (2001) *Curr. Opin. Struct. Biol.* **11,** 703–715
40. Komeili, A., and O'Shea, E. K. (2001) *Annu. Rev. Genet.* **35,** 341–364
41. Yamakasi, L., and Landford, R. (1992) in *Nuclear Trafficking* (Feldherr, C., ed), Academic Press, San Diego
42. Buchner, K. (2000) *J. Cancer Res. Clin. Oncol.* **126,** 1–11
43. Chen, R. H., Sarnecki, C., and Blenis, J. (1992) *Mol. Cell. Biol.* **12,** 915–927
44. Cyert, M. S. (2001) *J. Biol. Chem.* **276,** 20805–20808
45. Gama-Carvalho, M., and Carmo-Fonseca, M. (2001) *FEBS Lett.* **498,** 157–163
46. Lewis, J. M., Baskaran, R., Taagepera, S., Schwartz, M. A., and Wang, J. Y. (1996) *Proc. Natl. Acad. Sci. U. S. A.* **93,** 15174–15179
47. Perander, M., Bjorkoy, G., and Johansen, T. (2001) *J. Biol. Chem.* **276,** 13015–13024